Determining Addition Rates for the Growth of Uniform Silver Halide Crystals

David M. Ambrose [*] Connie Gerads Fournelle [†]
Katharine Gurski [‡] Danping Peng [§] Vivek Shekhar [¶]
Valsa Varghese [‖] Dr. David K. Misemer, Mentor [**]

July 31, 1998

1 Introduction

In photography, the quality of film is determined by the mean crystal size and the dispersity of sizes of the silver halide crystals in the film. A large crystal size provides a film with a fast speed, but the advantage of speed carries with it the disadvantage of a grainy image. Alternatively, small crystals will provide better resolution but require a longer exposure time. In order to achieve a specified film quality, we wish to make crystals with a given mean crystal size whose size dispersion is as small as possible.

Crystals are formed by beginning with an initial batch of silver halide seeds which are suspended in a gelatin solution. For our purposes, we have chosen to examine silver bromide. Solutions of $AgNO_3$ and KBr are then simultaneously added to the reactor through a double jet. The solution is mixed in a way to ensure that the Ag^+ and Br^- ions are evenly distributed

[*] Duke University
[†] University of Kentucky
[‡] University of Maryland
[§] UCLA
[¶] University of Cincinnati
[‖] University of Cincinnati
[**] 3M Corporate Research Laboratories

throughout the solution. The following chemical reaction takes place in the reactor:

$$Ag^+ + Br^- \rightleftharpoons AgBr$$

If the concentrations of ions in solution exceed the reaction's equilibrium concentration, $AgBr$ will precipitate out of the solution, adding to the mass of $AgBr$ in crystal form. For further analysis of the precipitation process, see [6], [7] and [1].

If an emulsion chemist specifies a desired final distribution of created crystals, we want to identify the addition rates of solutions necessary to achieve that distribution. We concentrate our efforts on the case where we start with an initial distribution of crystal seeds. We also offer a preliminary investigation of the formation of these seeds.

Upon completion of the crystal precipitation we want to be able to answer four questions about the crystal population. We are interested in the amount of material that has precipitated into crystals, as well as the mean crystal size, and the standard deviation in crystal size. We also seek information about the skewness of the distribution.

2 Model of Crystal Growth

The crystals grow through diffusion of solute from supersaturated solution to crystal surface and through the integration of the solute into the crystal lattice. We incorporate both of these mechanisms for growth into our model. We base our growth rate model on the results of Wey and Strong [7]. We describe the growth rate of the crystal as a function of the length of the crystal, ℓ, as

$$G(\ell, C_\infty, C_e) = \frac{K_i(C_\infty - C_e)(1 - \frac{L^*(C_\infty, C_e)}{\ell})}{1 + \varepsilon\ell}, \tag{1}$$

where K_i is the rate constant for the surface integration step, C_∞ is the concentration of dissolved silver, Ag, C_e is the equilibrium concentration of Ag in solution, and ε is the ratio of relative resistance of bulk diffusion to surface integration.

L^* is a reference length that describes when Ostwald ripening occurs; that is, when $\ell < L^*$ the crystal will dissolve.

We can get an approximation to L^* by

$$L^* \approx \frac{\Gamma_D}{\frac{C_\infty}{C_e} - 1}, \tag{2}$$

where Γ_D is a constant which depends on surface energy of the crystal per unit volume, molecular volume of the crystal and temperature.

We can characterize the distribution of crystal sizes, $\phi(\ell, t)$ by the PDE

$$\frac{\partial(G\phi)}{\partial \ell} + \frac{\partial \phi}{\partial t} = N(\ell, t), \tag{3}$$

where $N(\ell, t)$ refers to the nucleation rate, which is the rate of the new crystals being formed.

From the equilibrium state of the solution we can define

$$M_{Ag}^{soln} = M_{Ag}^{soln\ eq} + \Delta M, \tag{4}$$

where M_{Ag}^{soln} refers to the molar mass of Ag in solution, $M_{Ag}^{soln\ eq}$ is the molar mass of Ag in the solution at equilibrium, and ΔM is the change in the molar mass of the crystal.

Similarly, we have an equation for the equilibrium of bromide, Br, as

$$M_{Br}^{soln} = M_{Br}^{soln\ eq} + \Delta M. \tag{5}$$

We have a relationship between the amount of Ag and Br in the solution at equilibrium

$$\frac{M_{Ag}^{soln\ eq}}{V_R} \cdot \frac{M_{Br}^{soln\ eq}}{V_R} = k_{sp} \tag{6}$$

where k_{sp} is the solubility product of $AgBr$ [9].

Also, using conservation of molar mass we can describe the change of molar mass of Ag in the solution as

$$\begin{aligned} \frac{d}{dt} M_{Ag}^{soln} &= A_{Ag}(t) - \rho \int_0^\infty \frac{\partial \phi}{\partial t} \ell^3 d\ell \\ &= A_{Ag}(t) - 3\rho \int_0^\infty G\phi \ell^2 d\ell - \rho \int_0^\infty N(\ell, t) \ell^3 d\ell. \end{aligned} \tag{7}$$

where A_{Ag} is the addition rate of Ag into the system, $\rho \int_0^\infty \frac{\partial \phi}{\partial t} \ell^3 d\ell$ represents the rate of Ag taken from the solution and added to the mass of the crystal, and ρ is equal to the molar density of the $AgBr$ molecules in the crystal.

We have a complementary equation for the change of molar mass of bromide

$$\begin{aligned}\frac{d}{dt}M_{Br}^{soln} &= A_{Br}(t) - \rho\int_0^\infty \frac{\partial\phi}{\partial t}\ell^3 d\ell \\ &= A_{Br}(t) - 3\rho\int_0^\infty G\phi\ell^2 d\ell - \rho\int_0^\infty N(\ell,t)\ell^3 d\ell. \end{aligned} \tag{8}$$

with A_{Br} representing the addition rate of Br into the system.

Since we are adding Ag and Br in solution to our reactor, we are changing the volume of solution in the reactor by

$$\frac{dV_R}{dt} = \frac{A_{Ag}(t)}{N_{Ag}} + \frac{A_{Br}(t)}{N_{Br}}, \tag{9}$$

where N_{Ag} is the normality of the added $AgNO_3$ and N_{Br} is the normality of the added KBr solution.

We note that we can write the concentrations C_∞ and C_e in terms of M_{Ag}^{soln} and $M_{Ag}^{soln\ eq}$,

$$C_\infty = \frac{M_{Ag}^{soln}}{V_R}, \tag{10}$$

and

$$C_e = \frac{M_{Ag}^{soln\ eq}}{V_R}. \tag{11}$$

Values for the following constants can be found in [7] and [6]

$$\begin{aligned} K_i &= 2.322\times 10^4 \frac{cm^4}{mol\ min}, \\ \Gamma_D &= 5.7\times 10^{-7} cm, \\ \varepsilon &= 1.6\times 10^5 cm^{-1}, \\ \rho &= 0.0345\frac{mol}{cm_3}, \\ k_{sp} &= 7.825\times 10^{-14}\frac{mol^2}{cm^6}. \end{aligned}$$

3 Numerical Methods to Solve the PDE and System of ODEs

We can solve

$$\frac{\partial(G\phi)}{\partial \ell} + \frac{\partial \phi}{\partial t} = 0 \tag{12}$$

with the finite difference method. This equation is a conservation law. The simplest method for solving a conservation equation is the Lax-Friedrichs scheme

$$\phi_i^{n+1} = \frac{1}{2}(\phi_{i+1}^n + \phi_{i-1}^n) - \frac{\Delta t}{2\Delta x}[(G\phi)_{i+1} - (G\phi)_{i-1}], \tag{13}$$

which is a first order method. The system of ODEs that describe V_R (9), M_{Ag} (7), and M_{Br} (8) can be solved by the forward Euler method. Our calculations show that this method introduces too much dissipation, which tends to flatten out the peaks in our distribution ϕ. See Fig 1.

There are higher order schemes for conservation laws, such as ENO schemes [8] and WENO [3] schemes. In our calculation, a third order ENO scheme is used in the spatial differentiation, coupled with a third order Runge-Kutta time stepping method. The presentation here follows the presentation in [2], with some simplification.

The main steps of this scheme are described below applied to a general conservation law of the form:

$$u_t + F(u)_x = 0 \tag{14}$$

1. Compute the difference table.

$$\begin{aligned} D^1 F_i = &\quad F(u_{i+1}) - F(u_i) \\ D^2 F_i = &\quad F(u_{i+1}) - 2F(u_i) + F(u_{i-1}) \end{aligned}$$

2. If $\frac{F(u_{i+1})-F(u_i)}{u_{i+1}-u_i} > 0$, let $k = i$; Else, let $k = i+1$.

3. If $D^1 F_{k-1} < D^1 F_k$, then $c = D^1 F_{k-1}, k^* = k-1$; Else $c = D^1 F_k, k^* = k$.

4. If $D^2 F_{k^*} < D^2 F_{k^*+1}$, then $c^* = D^2 F_{k^*}$; Else $c^* = D^2 F_{k^*+1}$.

5. Let $\hat{F}_{i+\frac{1}{2}} = F(u_k) + c(i - k + \frac{1}{2}) + \frac{1}{2}(c^*(i-k^*)^2 - \frac{1}{3})$;

6. Approximate $F(u)_x$ by $\frac{F_{i+\frac{1}{2}} - F_{i-\frac{1}{2}}}{\Delta x}$.

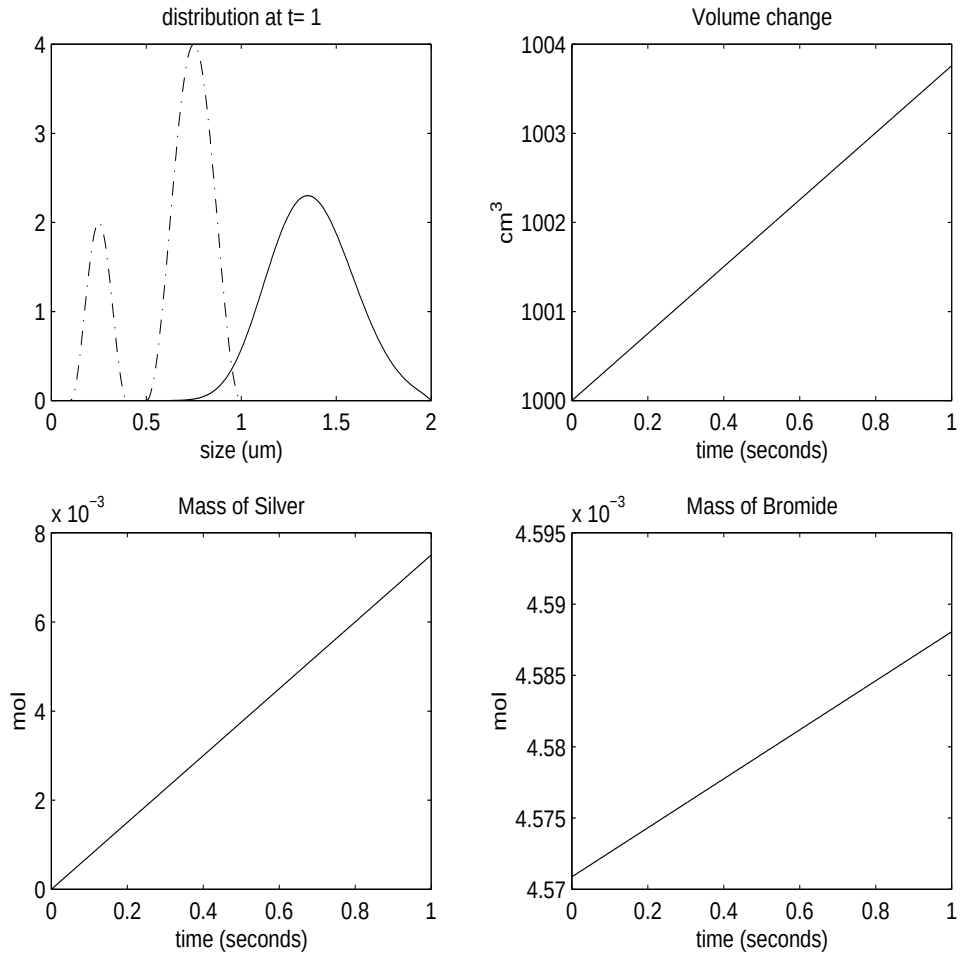

Figure 1: Results computed with Lax-Friedrichs Scheme. 256 grid points.

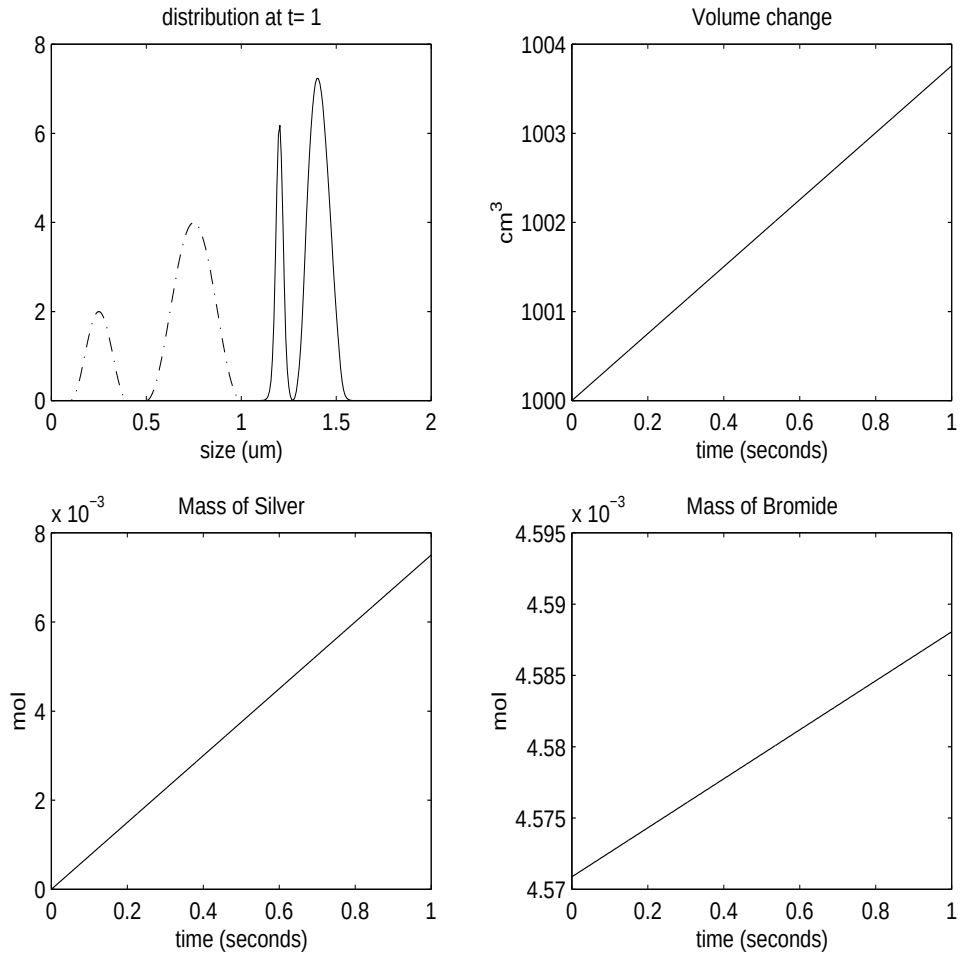

Figure 2: Results computed with ENO3-RK3. 256 grid points.

See Fig 2 for comparison with results computed with Lax-Friedrichs. Alternatively, we can rewrite equation (12) as

$$G\frac{\partial(\phi)}{\partial \ell} + \frac{\partial \phi}{\partial t} = -\frac{\partial G}{\partial \ell}\phi. \tag{15}$$

Along the characteristic curve, we have the system of ODEs

$$\begin{aligned} \frac{\partial \ell}{\partial t} &= G(\ell, C_\infty, C_e) \\ \frac{\partial \phi}{\partial t} &= -\frac{\partial G}{\partial \ell}\phi \end{aligned} \tag{16}$$

This system of ODEs given above coupled with the ODEs that describe V_R (9), M_{Ag} (7), and M_{Br} (8), can be solved by an ODE solver such as a third order Runge Kutta method. We have found that as the distribution becomes more steep the growth rate increases, which makes the system of ODEs very stiff. Therefore, a small time step must be used to insure stability. See Fig 3 for results.

4 Method of Characteristics without Nucleation

Consider again the PDE (12), which models the distribution of crystal sizes in the absence of nucleation. Recall equation (1) which defines the function G. If we hold C_∞ and C_e constant, then G becomes a function of ℓ alone. In this case, it is not difficult to solve the PDE by the method of characteristics. The solution is

$$\phi(\ell, t) = \frac{1}{G(\ell)} f(\psi(\ell, t)),$$

where f is an arbitrary (differentiable) function, and $\psi(\ell, t)$ (for $(\ell > L^*)$) is given by

$$\psi(\ell, t) = (1 + \varepsilon L^*)(\ell - L^*) + L^*(1 + \varepsilon L^*) \cdot \ln(\ell - L^*) + \frac{\varepsilon(\ell - L^*)^2}{2} - gt,$$

where $g = K_i(C_\infty - C_e)$.

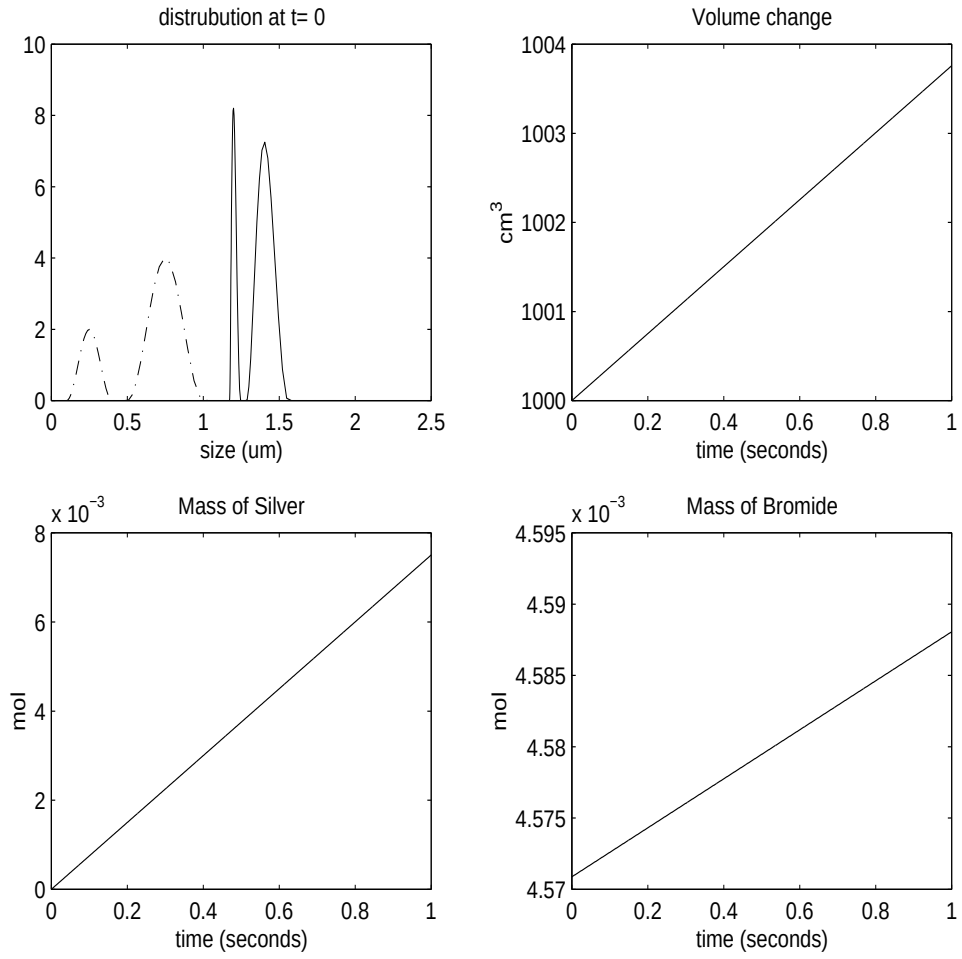

Figure 3: Results computed along the characteristics with RK3.

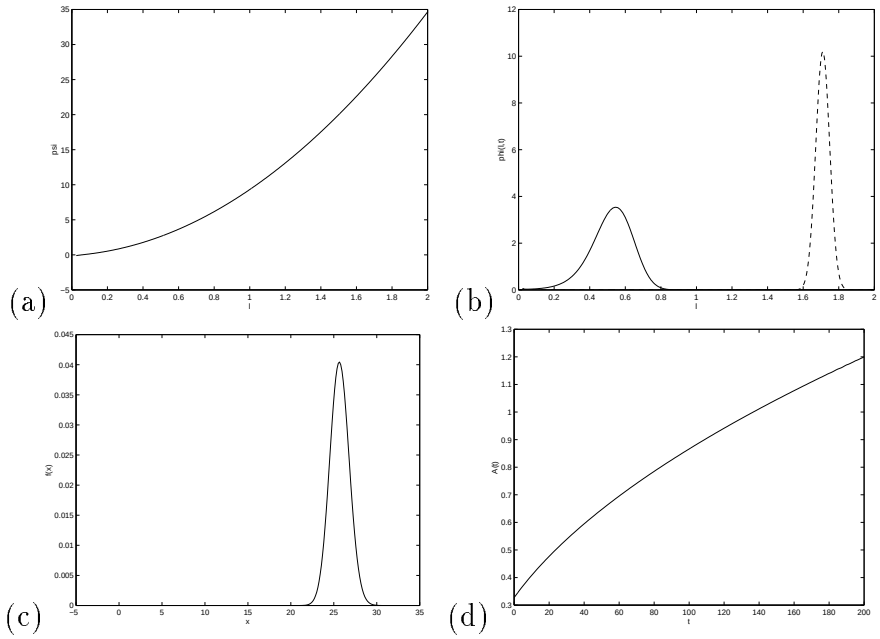

Figure 4: (a) ψ vs ℓ, (b) Final and Initial Distributions, (c) Arbitrary Function, f, (d) Addition Rate of $AgNO_3$

As Figure (4a) illustrates, ψ (for a given t) is invertible. This leads to a method of finding the unknown function f in the event that we wish to create an emulsion resulting in a given final distribution, $\phi(\ell, t_{end})$. That is, we define

$$f(x) = \phi({\psi_{t_{end}}}^{-1}(x), t_{end}),$$

where $\psi_t(\ell) = \psi(\ell, t)$. After computing f in this manner, we now compute

$$\phi(\ell, 0) = \frac{1}{G(\ell)} f(\psi(\ell, 0)).$$

We must be careful, however, in computing $\phi(\ell, 0)$ for a given t_{end}. Since we are operating in the absence of nucleation, we must be sure when solving for the initial condition that the same number of crystals are present in the beginning and end of the reaction. This may be restated as

$$\int_{L^*}^{\infty} \phi(\ell, 0) d\ell = \int_{L^*}^{\infty} \phi(\ell, t_{end}) d\ell.$$

For large values of t_{end}, these integrals will be unequal, owing to Ostwald ripening.

To find an upper bound on the size of t_{end}, we increase the size of t_{end} (starting at 1 minute) and compute the above integrals numerically. When the integrals differ by as much as one percent, we reason that Ostwald ripening has begun to occur and we estimate that t_{end} can be at most the previous value. The maximum t_{end} will depend on C_e, C_∞, and $\phi(\ell, t_{end})$.

Once we have computed $\phi(\ell, t)$ from our final desired distribution back in time to the initial seed distribution we can calculate the amount of $AgNO_3$ and KBr needed to be added to the system and their addition rates. Since we have held C_∞ and C_e we can rewrite the addition rate for silver as

$$A_{Ag}(t) = 3\rho\, Z \int_0^{\infty} G(\ell, C_\infty, C_e)\, \phi(\ell, t)\, \ell^2\, d\ell, \tag{17}$$

where

$$\begin{aligned} Z &= \frac{1}{1 - \frac{C_\infty}{N_{Ag}} - \frac{C_\infty \cdot U}{N_{Br}}}, \\ U &= \frac{1 + \frac{C_\infty}{N_{Ag}} - \frac{C_\infty}{N_{Ag}}}{1 + \frac{C_\infty}{N_{Br}} - \frac{Q}{N_{Br}}}, \\ Q &= \frac{k_{sp}}{C_e} + C_\infty - C_e. \end{aligned}$$

The addition rate for bromide is

$$A_{Br}(t) = A_{Ag}(t)\,U. \tag{18}$$

For example, suppose a chemist wants to create the final (dashed) distribution in Figure (4b). We calculate f as described above; this is displayed in Figure (4c). From here we may calculate the initial distribution for various values of t_{end}. This yields a maximum t_{end} of about 200 minutes, and the initial distribution in Figure (4b). Finally, we are able to calculate (since we know now $\phi(\ell, t)$ for various values of t) the addition rates; the addition rate function for silver is shown in Figure (4d).

5 Method of Characteristics with Nucleation

Next we consider the issue of nucleation; that is, rather than concentrating on increasing the crystal size with a distribution of prepared crystal seeds, we will be creating these crystal seeds from solution. Silver halide nuclei are formed by spontaneous nucleation that is triggered when the supersaturation ratio, S, exceeds a certain threshold. To create a distribution of seeds of fairly uniform size, the time during which nucleation occurs must be relatively short. The behavior of S can be seen in figure (5). There is a quick transition to the period of crystal growth where the supersaturation ratio remains approximately constant and low enough to avoid the formation of additional crystals [4] [5].

We will refer to the initial phase of the precipitation experiment as the nucleation region. In this region we raise $S(t)$ from zero to above the nucleation threshold, S_c to a maximum S_m and then smoothly lower $S(t)$ to S_c. The second phase of the experiment, which we call the transition phase, lowers $S(t)$ from S_c to the optimal value of the supersaturation ratio for crystal growth, S_g. We determine S_g by a numerical scheme based on the method of characteristics for the third phase, the growth region.

When we solved equation (3) with $N(\ell, t) = 0$ by the method of characteristics for the growth region we assumed that C_∞ and C_e remained constant. This is a reasonable approximation given that the supersaturation ratio can be held constant while sustaining crystal growth. However, during nucleation S varies with time as described above. We can design an experiment to hold C_e constant through all three regions while varying C_∞ to achieve our change

Figure 5: Supersaturation ratio versus time from Leubner, 1987

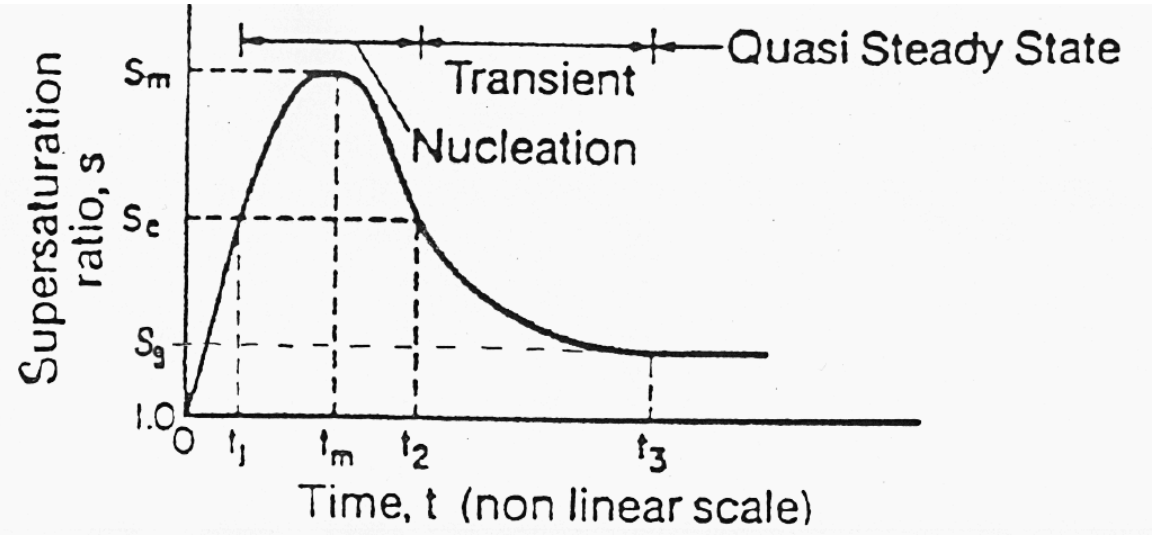

in $S(t)$. We define C_e to take the optimal value, determined by the method of characteristics, for the growth region.

To determine the addition rates for Ag and Br for the nucleation and transition regions we return to the method of characteristics. We have $\psi(\ell, t)$ is a solution of

$$\frac{d\ell}{dt} = G(\ell, C_e, C_\infty) = \frac{K_i C_e(\ell(S(t) - 1) - \Gamma_D)}{\ell + \epsilon\ell^2}, \tag{19}$$

which can be found numerically for a given $S(t)$. The optimal $S(t)$ for the nucleation and transition phases will be chosen by a combination of the method by which the optimal choices for C_e and C_∞ were chosen for the growth region and experimental numerical tests with the addition rates to determine an appropriate value for S_m.

Using the empirical theory of spontaneous nucleation of spherical crystals to create a nucleation rate for the model, we have

$$N(\ell, t) = J\, V_R(t)\, \delta(\ell - \ell_0) = A\, \left(\exp(\frac{-\pi\Gamma_D^3 R_g^3}{12k^2(\ln S(t))^2})\right) V_R(t)\, \delta(\ell - \ell_0), \tag{20}$$

where ℓ_0 specifies our nucleated crystal size, R_g is the universal gas constant, k is Boltzmann's constant, and A is a constant on the order of 10^{23} to $10^{32.5}$. Numerical experiments should help to determine the proper value for A.

Thus the solution to (3) can be written

$$\phi(\ell,t) = \frac{1}{G(\ell,\psi(\ell,t))}\left(\frac{J\,V_R(t)}{G(\ell_0,\psi(\ell_0,t))^2} + f(\psi(\ell,t))\right). \tag{21}$$

With this formula an emulsion chemist may specify a desired final crystal size distribution and we will be able to determine the necessary addition rates for silver and bromide using our numerical algorithm. Since we have specified our final distribution we will know, without new calculations, the final mass in crystals, the mean size of the crystal grains, the dispersion of the grain sizes, and the skewness of the distribution.

6 Conclusion

Two different approaches were investigated for the problem of creating crystals with a given mean crystal size and with the dispersity of size as small as possible. The first approach uses analysis, in particular, the method of characteristics. Given the final desired crystal size distributions by the emulsion chemist, in the absence of nucleation we were able to determine the initial crystal size distribution and the addition rates of Ag^+ and Br^-.

We also theoretically determined how to make the initial seeds and obtained the formula for computing the addition rates of Ag^+ and Br^- when nucleation was taken into account.

In the second approach, numerical methods were investigated and their results were compared. Starting with the initial seed distributions with suitable addition rates, we were able to capture the final crystal size distributions. The numerical methods used were: Lax-Friedrichs first order finite difference scheme coupled with first order ODE solvers, the higher order finite difference scheme ENO together with RK3 as the ODE solver, and using characteristics with RK3 as the time stepping method for the numerics.

Further, both approaches answered the four questions about crystal population. We were able to determine the total mass of crystals, the mean size of a crystal grain, the dispersion of grain sizes, and the skewness of the distribution.

References

[1] Daniel D.F.Shiao. Kinetic modeling of growing silver halide microcrystals in gelatin solution. *Photographic Science and Engineering*, 24(5):227–231, 1980.

[2] R.P. Fedkiw, B. Merriman, R. Donat, and S. Osher. The penultimate scheme for systems of conservation laws: Finite difference ENO with marquina's flux splitting. *UCLA CAM Report*, 96-18, 1996.

[3] G-S.Jiang and C.W. Shu. Efficient implementation of weighted ENO schemes. *Journal of Computational Physics*, 126:202–228, 1996.

[4] Ingo H.Leubner. Crystal formation (nucleation) under kinetically controlled and diffusion-controlled growth conditions. *The Journal of Physical Chemistry*, 91(23):6069–6073, 1987.

[5] I.H.Leubner, R.Jagannathan, and J.S.Wey. Formation of silver bromide crystals in double-jet precipitation. *Photographic Science and Engineering*, 24(6):268–272, 1980.

[6] J.S.Wey and R.W.Strong. Growth mechanism of AgBr crystals in gelatin solution. *Photographic Science and Engineering*, 21(1):14–18, 1977.

[7] J.S.Wey and R.W.Strong. Influence of the Gibbs-Thomson effect on the growth behavior of AgBr crystals. *Photographic Science and Engineering*, 21(5):248–252, 1977.

[8] C.W. Shu and S. Osher. Efficient implementation of essentially non-oscillatory shock capturing schemes II. *Journal of Computational Physics*, 83:32–78, 1989.

[9] Lars Gunnar Sillen and Arthur E. Martell, editors. *Stability Constants of Metal-Ion Complexes*. The Chemical Society, Burlington House, London, 1964.